AIP | Journal of Applied Physics

Realistic performance prediction in nanostructured solar cells as a function of nanostructure dimensionality and density

I. Tobías, A. Luque, E. Antolín, P. García-Linares, I. Ramiro et al.

Citation: J. Appl. Phys. **112**, 124518 (2012); doi: 10.1063/1.4770464

View online: http://dx.doi.org/10.1063/1.4770464

View Table of Contents: http://jap.aip.org/resource/1/JAPIAU/v112/i12

Published by the American Institute of Physics.

Realistic performance prediction in nanostructured solar cells as a function of nanostructure dimensionality and density

I. Tobías,[a] A. Luque, E. Antolín, P. García-Linares, I. Ramiro, E. Hernández, and A. Martí
Instituto de Energía Solar–Universidad Politécnica de Madrid, ETSI Telecomunicación–Ciudad Universitaria, 28040 Madrid, Spain

(Received 21 June 2012; accepted 27 November 2012; published online 28 December 2012)

The behavior of quantum dot, quantum wire, and quantum well InAs/GaAs solar cells is studied with a very simplified model based on experimental results in order to assess their performance as a function of the low bandgap material volume fraction f_{LOW}. The efficiency of structured devices is found to exceed the efficiency of a non-structured GaAs cell, in particular under concentration, when f_{LOW} is high; this condition is easier to achieve with quantum wells. If three different quasi Fermi levels appear with quantum dots the efficiency can be much higher. © *2012 American Institute of Physics*. [http://dx.doi.org/10.1063/1.4770464]

I. INTRODUCTION

The use of low dimensional nanostructures in the absorber region of a solar cell was proposed some years ago as a means of increasing the efficiency.[1] Today, an important application of quantum wells (QWell) is adjusting the bandgap in multi-junction (MJ) solar cells. Metamorphic triple junction solar cells allow some lattice mismatch for achieving a better spectral adaptation,[2,3] but this entails a reduction of the crystal quality that favors the efficiency of the less spectrum-adapted latticed-matched solar cells.[4] An option under consideration is to use a material system where this effect can be avoided, such as with InP-based multijunction solar cells.[5] Another approach is to use nanostructures, QWell but also quantum dot (QD) solar cells,[6] to trim the bandgap of the cells to the optimum values.

Only two electron quasi Fermi levels (QFLs) are postulated (for the valence and conduction bands (CB)) so that these cells are subject to the detailed balance efficiency limits of conventional solar cells.[7,8]

The intermediate band solar cell (IBSC) was proposed[9] as a way of breaking the detailed balance efficiency limits of conventional solar cells. It was suggested to use the confined levels of quantum dots as intermediate band;[10] in this way prototype devices have been fabricated by including InAs QDs in a GaAs solar cell.[11–14] In this concept, it is essential that electrons in the confined, gap states of the dots are not in equilibrium with those in the bands, that is, in operation the Fermi level splits into three separated QFLs. To our knowledge, this happens today in experimental devices only at low temperature.[15–17] The cells show a small sub bandgap current contribution because they contain a small number of QDs, but sensible voltage degradation at room temperature occurs and hence their efficiency is low.

The purpose of this paper is to explain the influence of the density of low dimensional structures on the behavior of solar cells with simplest models in a quest for clarification that allows comparing nanostructures of different dimensionality. These models differ from the detailed balance model widely used so far[7,9,18] in that light absorption and recombination are in agreement with experimental results instead of assuming full absorption of the sub-bandgap photon flux, occurring in very thick devices which are unpractical and unfeasible. Furthermore in the detailed balance models the recombination is assumed to be only radiative while in this paper the recombination is dominated by non-radiative recombination in the range of the one actually observed. The model used is presented in Sec. II along with the parameters adopted. Then, in Sec. III, calculations are done for different structures for variable light concentration, doping and quantum dot density. Section IV contains the most relevant conclusions of the work.

II. MODELS AND PARAMETERS

In this study, we will compare the behavior of GaAs solar cells containing different InAs nanostructures, a material system that has been extensively used for the formation of nanostructures in semiconductor devices; however, not all the structures we propose in the article can surely be realized with it due to technological reasons. In addition to the homogeneous cell, devices containing quantum dots, wires, and wells will be analyzed. The dimensions involved are explained in Figure 1. Relevant data concerning the materials and geometry are collected in Table I.

In order to establish proper comparison among the different nanostructures, they will be classified according to the relative volume of well material, f_{LOW}, they contain. For QD structures with N_{QD} dots per unit volume, $f_{LOW} = N_{QD}abc$; for quantum wire (QWire) structures $f_{LOW} = N_{QWire}ab$ with N_{QWire} wires per unit area; and $f_{LOW} = N_{QWell}c$ for N_{QWell} QWells per unit length. These relationships between the content of well material and the nanostructure density are illustrated in Figure 2. The maximum dot density that makes sense is $N_{QD} = 1/abc = 6.51 \times 10^{17}\,\mathrm{cm}^{-3}$, corresponding to 100% homogeneous well material. However, when the wavefunctions of the well states overlap and they become extended and minibands can form. This transition from isolated structures to

[a]Author to whom correspondence should be addressed. Electronic mail: tobias@ies-def.upm.es. Telephone: + 34 91 4533550. Fax: +34 91 5446341.

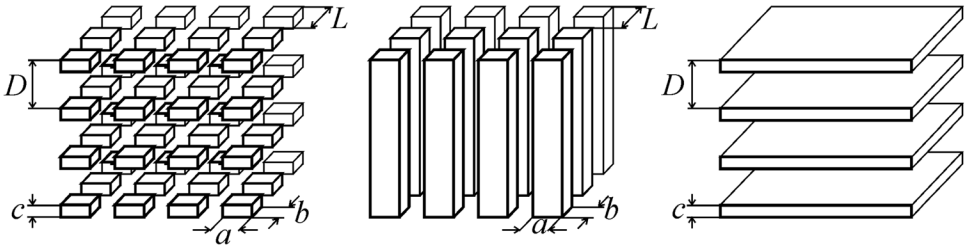

FIG. 1. Confinement structures (quantum dots, wires, and wells) with dimensions.

the homogeneous material has not been modelled as it opens a lot of different possibilities. For instance, increasing the density of dots can lead to wire or well formation, etc. A density limit can be estimated as follows. The penetration depth of nanostructure wavefunctions into the barrier material for the deepest lying states is 1.13 and 1.25 nm in horizontal and vertical directions, respectively, so that the onset for homogeneous material is calculated to be produced at an equivalent quantum dot density of around $5 \times 10^{17}\,\mathrm{cm}^{-3}$ which is used in this paper as a value representative of the high nanostructure density limit.

In order to calculate generation and recombination in the structures, the carrier concentrations must be derived as a function of the externally applied voltage. It will be considered that the electrons in the different potential wells (dots, wires, or wells) are in equilibrium among them and (except when explicitly stated) with the conduction band of the barrier material. Equilibrium between confined and conduction electrons has been found in prototype InAs/GaAs QD-IBSCs except at low temperatures[15] due to thermal photons and, most often, also due to tunneling. On the other hand, the continuous nature of the density of states in wires and wells makes it difficult to think of different Fermi levels.

In these conditions, for the three cases in Figure 1, the electron concentration as far as charge density and recombination are concerned is the sum of extended and confined electron concentrations

$$\begin{aligned} n &= n_{CB} + n_{0D}, \\ n &= n_{CB} + n_{1D}, \\ n &= n_{CB} + n_{2D}, \end{aligned} \tag{1}$$

where n_{CB} is the free electron concentration in the CB of the barrier material, and n_{0D}, $n_{1D,}$ and n_{2D} the concentration of electrons in dot, wire, or well states. Although not actually true,[19] the valence band (VB) is assumed not to be affected by the nanostructure because the influence in the problem studied here is thought to be a minor effect; thus $p = p_{VB}$. Besides, the effect of the potential step on the extended states of the conduction band is also neglected and the density of states of the barrier material is assumed.

These values are calculated from the position of the Fermi levels with the usual formulas[20]

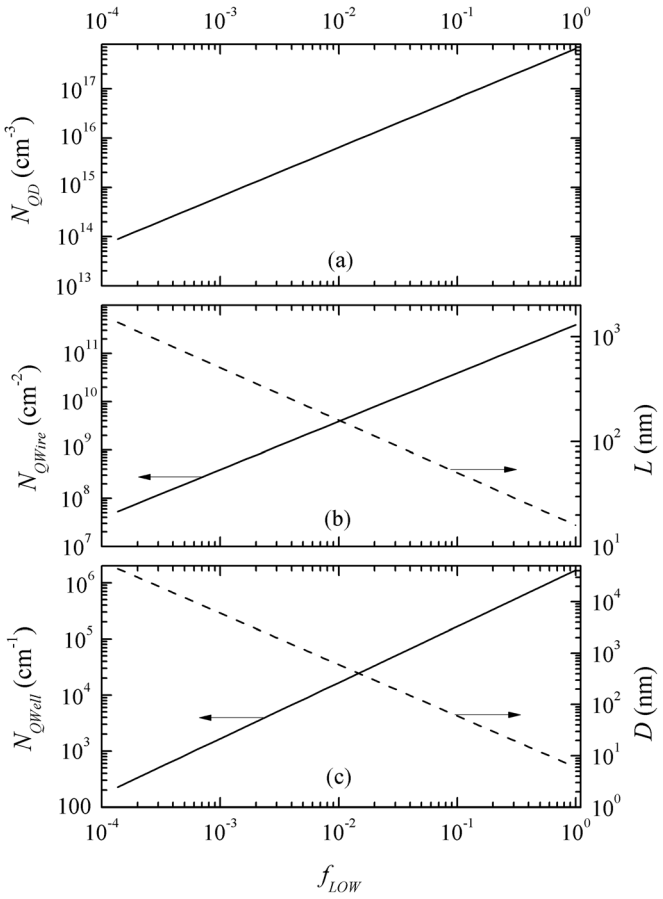

FIG. 2. Density of nanostructures and separation between them as a function of low bandgap material content, f_{LOW}, for (a) quantum dots, (b) wires, and (c) wells. D and L are defined in Figure 1.

TABLE I. Parameters.

Parameter	Value
GaAs conduction band effective density of states N_C (300 K)	$4.2 \times 10^{17}\,\mathrm{cm}^{-3}$ (Ref. 32)
id. for the valence band N_V (300 K)	$1.4 \times 10^{19}\,\mathrm{cm}^{-3}$ (Ref. 32)
GaAs bandgap E_G	1.424 eV (Ref. 32)
Conduction band offset qV_0	0.473 eV (Ref. 21)
InAs effective mass m[a]	0.0294 m_0 (Ref. 21)
Vertical dimension of QDs and wells c	6 nm (Ref. 21)
Lateral dimensions of QDs and wires a, b	16 nm (Ref. 21)
Donor level $E_C - E_D$	0.006 eV (Ref. 33)
Recombination lifetime τ	10 ns[a]
Conventional photocurrent J_{LBG}	$25\,\mathrm{mA \cdot cm}^{-2}$[a]
Ratio of sub bandgap to bandgap photons in AM15D for quantum dots	0.484[b]
id. quantum wires	0.649[b]
id. quantum wells	0.547[b]
id. Homogenous well material	0.777[b]
Optical cross section for subbandgap states σ_0	$4.7 \times 10^{-15}\,\mathrm{cm}^2$[a]
Cell thickness W	1 μm

[a]Estimated from experimental devices.
[b]Calculated.

$$n_{CB} = N_C(T) \times F_{1/2}\left(\frac{E_{Fn} - E_C}{k_B T}\right),$$
$$p = N_V(T) \times F_{1/2}\left(\frac{E_V - E_{Fp}}{k_B T}\right), \quad (2)$$

$$n_{0D} = \frac{2}{L^2 D}\sum_k \frac{g_k}{1 + \exp\left(\frac{E_k - E_{Fn}}{k_B T}\right)}, \quad (3)$$

$$n_{1D} = \frac{2}{L^2}\sqrt{\frac{2m^* k_B T}{\hbar^2 \pi}}\sum_k g_k \times F_{-1/2}\left(\frac{E_{Fn} - E_k}{k_B T}\right), \quad (4)$$

$$n_{2D} = \frac{2}{L^2}\frac{m^* k_B T}{\hbar^2 \pi}\sum_k g_k \ln\left(1 + \frac{E_{Fn} - E_k}{k_B T}\right), \quad (5)$$

$F_j(\eta) \equiv \frac{1}{\Gamma(j+1)}\int_0^\infty \frac{x^j dx}{1+\exp(x-\eta)}$ is a Fermi-Dirac integral. E_k denotes the energy level of the QD or the energy threshold for wires and wells and g_k its degeneracy. These levels are calculated with the simplified model described in Ref. 21 and are shown in Table II.

Carrier concentrations as a function of voltage are calculated by imposing charge neutrality in the cell bulk.[22] This condition along with the equality of QFLs separation to the external voltage allows relating the electron and hole concentrations with the voltage,

$$p + N_D^+ - n = 0,$$
$$E_{Fn} - E_{Fp} = qV. \quad (6)$$

Here, $N_D^+ = \frac{N_D}{1+\exp\left(\frac{E_{Fn}-E_D}{k_B T}\right)}$ is the concentration of ionized donors. The donor concentration is in general set equal to the quantum dot density so that the fundamental level is half filled at zero bias, as is advised for QD-IBSCs (although this might not be the optimum).[9,22] For the rest of the nanostructures, Figure 2(a) is to be used to determine the doping as a function of f_{LOW}.

We will assume that the electron-hole recombination rate is proportional to the hole density. Then, if the valence band is not degenerate, the net recombination rate per unit volume can be written as

$$U = \frac{p - p_0}{\tau}, \quad (7)$$

where p_0 is the equilibrium hole density and τ the recombination lifetime. This simple law is frequently obeyed in n-type material under low injection conditions and will be supposed to hold in all the cases in this paper, without distinction as to whether the recombining electrons are in confined or extended states.[23] The lifetime is related to one or several defects that act as recombination centers by introducing deep levels. These traps are present even in nonstructured semiconductors but strain relaxation in InAs/GaAs nanostructures can produce them; in these paper, however, we assume the lifetime to be independent on the density of nano-sized features. If the carrier densities are uniform across the cell of thickness W and we assume that this recombination mechanism is dominant in the cell, the recombination current density is

$$J_R = qW\frac{p - p_0}{\tau}. \quad (8)$$

Lack of fulfillment of the uniform density of carriers assumption would result in a modified effective lifetime.

The cell net current can be written as the balance between generation and recombination. The generation current density J_L has two components: the conventional one J_{LBG} resulting from the valence to conduction band transitions plus a sub bandgap contribution J_{LSBG} due to transitions from the valence band to confined states,

$$J_L = J_{LBG} + J_{LSBG} = Q\left(J_{LBG(\max)} + J_{LSBG(\mathrm{abs})}\right)$$
$$= QJ_{LBG(\max)}\left(1 + \frac{J_{LSBG(\max)}}{J_{LBG(\max)}}\frac{J_{LSBG(\mathrm{abs})}}{J_{LSBG(\max)}}\right). \quad (9)$$

If the absorption of photons over the bandgap is complete, a quantum efficiency is defined as $Q = J_{LBG}/J_{LBG(\max)}$, where $J_{LBG(\max)}$ is the maximum current density available to the barrier bandgap. This quantum efficiency is assumed to affect the sub bandgap absorption, which may not be complete so that $J_{LSBG(\mathrm{abs})} \le J_{LSBG(\max)}$, where $J_{LSBG(\max)}$ is the flux of incident photons with energies between the lowest nanostructure energy and the barrier gap, times the electron charge, i.e., the maximum current density that could be gained by absorption in the nanostructures. The fraction $J_{LSBG(\max)}/J_{LBG(\max)}$ is just a property of the spectrum and the gaps involved; it is given in Table I for the AM1.5 Direct spectrum for the nanostructures and also for the case of the 100% homogeneous well material. Finally, subbandgap absorption is modeled with an absorption coefficient α which is proportional to the density of empty subbandgap states. The photocurrent is thus written

$$J_L = J_{LBG}\left(1 + \frac{J_{LSBG(\max)}}{J_{LBG(\max)}}\left(1 - e^{-\alpha W}\right)\right)$$
$$\equiv J_{LBG}\left(1 + \frac{J_{LSBG(\max)}}{J_{LBG(\max)}}\left(1 - \exp\left(-\sigma_0 W N_{SBGempty}\right)\right)\right), \quad (10)$$

where σ_0 is an optical capture cross section whose value is determined by the fact that in experimental devices with around $4 \times 10^{16}\,\mathrm{cm}^{-3}$ quantum dots and $W = 0.1\,\mu\mathrm{m}$ an incremental photocurrent of around 1% has been measured.[11]

TABLE II. Energy levels. InAs/GaAs quantum structures. Lateral dimensions $a = b = 16$ nm; vertical $c = 6$ nm.

Energy level (from E_C) and degeneracy	Quantum dots	Quantum wires	Quantum wells
$E_C - E_1$ (eV) (g_1)	0.300 (1)	0.413 (1)	0.359 (1)
$E_C - E_2$ (eV) (g_2)	0.209 (2)	0.322 (2)	0.032 (1)
$E_C - E_3$ (eV) (g_3)	0.118 (1)	0.231 (1)	
$E_C - E_4$ (eV) (g_4)	0.056 (2)	0.169 (2)	
$E_C - E_5$ (eV) (g_5)		0.078 (2)	

We are then assuming that all structures present the same *average* cross section. Though it is to be expected that on averaging the differences are smoothed out, this of course introduces uncertainty and impedes to account for systematic deviations related to symmetry. Equation (10) also assumes that all empty states within the gap contribute equally to the current without regard to their energy position, just as if they were all located at the lowest energy: this approximation tends to overestimate the photocurrent more for structures with lower gap.

The *J-V* curve of the cell is obtained as follows. Since the quasi-Fermi level split is constant and equal to the external voltage, Eqs. (6) and (7), together with Eqs. (2)–(5), allow to determine the concentration of holes and of extended and confined electrons. The number of empty states in the gap is calculated as the total number of states—the integral of the corresponding density of states—minus the number of confined electrons $n_{0D,\ n1D,}$ or n_{2D}. The photogenerated current is then obtained from Eq. (10). The total electron concentration is used to obtain the recombination current (Eq. (8)). The net current $J=J_L$-J_R is then calculated as a function of voltage, and shortcircuit current, open circuit voltage and maximum power are derived without further approximation.

III. RESULTS AND DISCUSSION

Figure 3 plots the variation of the efficiency, the open circuit voltage, and the short circuit current density as a function of f_{LOW} for solar cells with nanostructures, without light concentration ($X=1$). All results shown are calculated for 300 K and for the same J_{LBG}, W, and σ_0. As a reference, a GaAs cell with a doping density equal to $N_D=5\times10^{17}\,\mathrm{cm}^{-3}$ is also represented. The nanostructured devices have either a fixed donor density $N_D=5\times10^{17}\,\mathrm{cm}^{-3}$ (label *H*) or a doping density which is equal to the QD density corresponding to f_{LOW} (label *V*). The former value is used for comparison with the reference cell, while equal doping and dot densities, as explained, are found in experimental devices whose performance we want to explain. In two quasi-Fermi level operation the role of doping is basically the same as in conventional devices, affecting directly the cell voltage.

As expected, the effect is negligible for all the nanostructures if f_{LOW} is very small, provided the doping is high. The reduction of voltage for the case of variable doping is mainly related to the decrease of dopant density.

Most QD cells have today a dot density ranging between 4×10^{15} and $4\times10^{16}\,\mathrm{cm}^{-3}$ (Refs. 11, 12, 24, and 25). Reductions of voltage below 0.8 V, as shown in the figure, are very common, but yet some cells present voltages close to their references,[26] sometimes near 1 V. This can be explained by a better recombination lifetime. It is also possible to find QD devices with a short circuit current increment of over 5% (Ref. 27) with respect to the reference cells, thus revealing the possibility of larger optical capture sections than assumed by us.

The world record efficiency for GaAs cells at one sun is today 28.1% (Ref. 28) with a current density of $29.4\,\mathrm{mA\cdot cm}^{-2}$ ($25\,\mathrm{mA\cdot cm}^{-2}$ in our reference cell) and a short-circuit voltage of 1.11 V (1.05 V in our reference cell). Our reference cell is indeed not a record device, but an easily obtainable cell that justifies the lifetime and current density values used in this paper. The reference—and the nanostructured cells—discussed here can, however, be improved by lifetime or short-circuit current density increases.

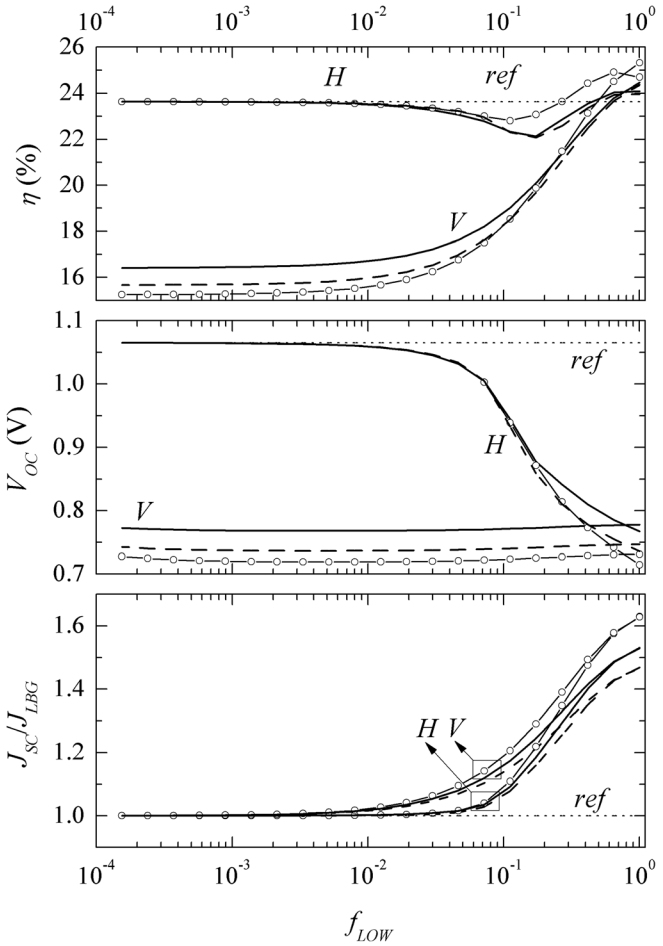

FIG. 3. From top to bottom, efficiency, open circuit voltage and short circuit current density (normalized to the reference photocurrent) as a function of well material content. Thick solid lines: quantum dot solar cells; dashed: quantum wells; line plus circles: quantum wires. Label *V*: variable doping $N_D=N_{QD}$; label *H*: high constant doping $N_D=5\times10^{17}\,\mathrm{cm}^{-3}$. Dotted line: uniform GaAs doped with $N_D=5\times10^{17}\,\mathrm{cm}^{-3}$. $X=1$.

QWell cells are usually manufactured with a larger equivalent density than that of the dots: above $10^{17}\,\mathrm{cm}^{-3}$ ($f_{LOW}=0.3$).[29] For this reason, they usually experience substantial current increases and they may be in the range in which the efficiency of the reference cell is actually exceeded.

The following graphs collected in Figure 4 show the effect of increasing light concentration (no series-resistance degradation considered) on nanostructured cells and on a homogeneous reference cell. Equal doping and dot densities are assumed, with two values referred to as high and low doping. In the high density case, wavefunction overlap maybe significant for quantum dots, so that the isolated nanostructure picture used here is approximate.

The open circuit voltage of structured cells is very similar for all dimensionalities and doping densities, but, in the case of low doping, low voltage is due to doping and, in the case of high doping, to high nanostructured material fraction. It increases logarithmically with concentration and the lines run

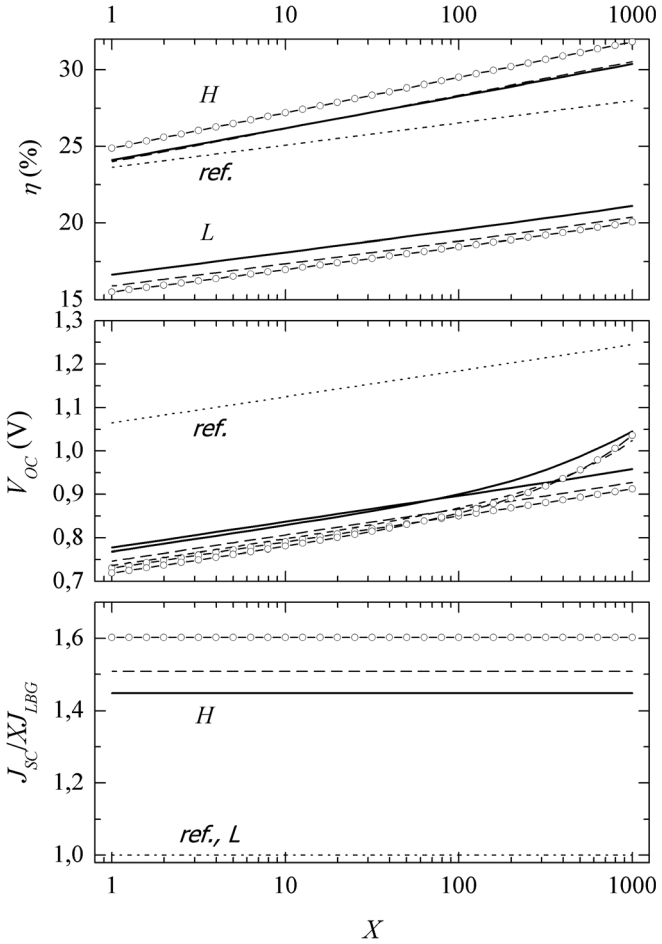

FIG. 4. From top to bottom, efficiency, open circuit voltage and short-circuit current density (normalized to the reference photocurrent) as a function of concentration. Thick solid lines: quantum dot solar cells; dashed: quantum wells; line plus circles: quantum wires. Label *L*: $N_D = N_{QD} = 5 \times 10^{15}\,\mathrm{cm}^{-3}$; label *H*: $N_D = N_{QD} = 5 \times 10^{17}\,\mathrm{cm}^{-3}$. Dotted line: uniform GaAs doped with $N_D = 5 \times 10^{17}\,\mathrm{cm}^{-3}$.

parallel except for the low doping cases at high X where the faster increase is related to the onset of the high injection regime and hence the failure of the underlying low injection assumption. As in Figure 4, wires present a lower voltage than wells, and these lower than dots. The reference cell voltage is much greater in all cases.

Current is proportional to concentration (note the normalization). In consequence, the variation of efficiency does not alter very much the order established at one sun: structures with more sub bandgap states perform better and, regarding confinement geometry, the order is reversed with respect to voltage (first dots, then wells, and finally wires).

Since current is better and voltage is similar, high doping—high nanostructure density samples present better efficiencies than lowly doped and engineered ones. Wells and dots are similar to and slightly worse than wires. The small advantage of nanostructured cells over the reference found at one sun increases with concentration. Again, in this case, the efficiency of the reference cell in our model is below that of the world record cell, the world record being 29.1% efficiency for concentrator cells at 117 suns.[28]

With the used data, the voltage loss due to gap states is offset by the sub bandgap current gain and still complies with the detailed balance limit,[6] but yet this is not the best to be expected by the use of nanotechnology. In effect, if disequilibrium can be sustained between confined and band states, the voltage can be recovered: this is at the heart of the intermediate band concept. Let us assume all states in the confined spectrum of the dot to be in mutual equilibrium,[30] with a quasi-Fermi level that lies ΔE_F ΔE_Fbelow the quasi-Fermi level of CB electrons. The confined states are not in contact with the external electrodes, so that they are, as a whole, open circuited—even if transport between them were allowed—and the net cell current density is the signed sum of bandgap and sub bandgap components, just as in the case studied before. However, now concentrations of electrons in band and confined states are ruled by different quasi-Fermi levels.

Figure 5 shows, for 1000× concentration, the influence of conduction-confined states quasi Fermi level split up to a maximum value $E_C - E_1 = 0.3\,\mathrm{eV}$. The efficiency experiences a sizeable increase in the two cases in the plot, but is most important if the QD density is high: about 100 times higher than that in present cells. We believe that increasing present concentrations 20 times is possible.[19] This would give efficiencies above 30%, already very attractive. Furthermore, the thickness of the nanostructured region can be increased from 1 to 5 μm with an effect approximately similar to the 100-fold increase in density.

The reason the splitting of the IB and conduction band quasi Fermi levels is not produced is because of the excited confined states within the GaAs bandgap. At room temperature they provide a ladder for the electrons from and to the IB.[23] Furthermore, beyond 56 meV, population inversion will take place between the conduction and the highest confined level so producing an additional effective path to keep the IB and the CB at the same quasi Fermi level. Smaller QDs and a larger material bandgap are necessary to avoid this important drawback.

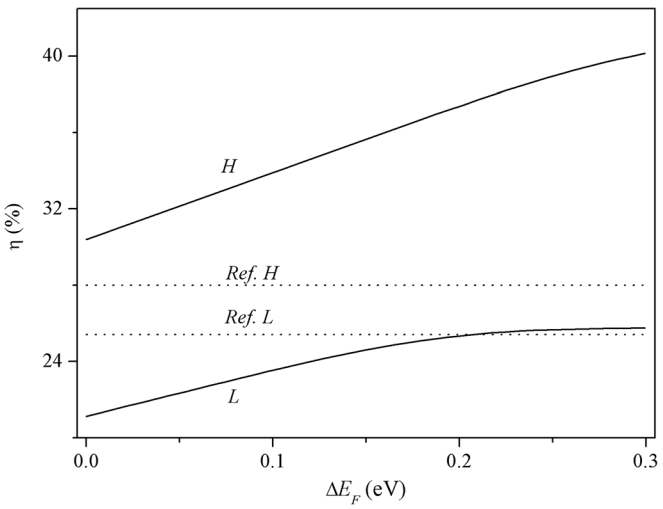

FIG. 5. Efficiency as a function of the quasi-Fermi level split between the CB and the QD states at $X = 1000$. Solid lines: quantum dot solar cells with $N_D = N_{QD} = 5 \times 10^{15}\,\mathrm{cm}^{-3}$ (L) and $N_D = N_{QD} = 5 \times 10^{17}\,\mathrm{cm}^{-3}$ (H). Dotted lines: uniform GaAs doped with $N_D = 5 \times 10^{17}\,\mathrm{cm}^{-3}$ (Ref. H) or $N_D = N_{QD} = 5 \times 10^{15}\,\mathrm{cm}^{-3}$ (Ref. L).

IV. CONCLUSIONS

Solar cells with quantum nanostructures of different dimensionality have been analyzed with a simple but realistic model, first under the assumption of thermal equilibrium between confined and free electrons and then removing this assumption.

It is found that the influence of the dimensionality on the cell performance (J_{SC}, V_{OC}, and efficiency) is not very acute and the most important parameters are the low bandgap material fraction f_{LOW} and the doping level. Good results are achieved when these are high. However, it is easier to achieve high f_{LOW} in quantum wells. In quantum dots both aspects are linked together because the doping level is usually similar to the QD density that is proportional to f_{LOW}. Anyway, quantum wires tend to give somewhat higher efficiency, dots and wells being very similar for the same f_{LOW}.

At one sun, under this high density, the nanostructured efficiency can slightly exceed the bulk cell efficiency. This result assumes that the lifetime is the same in nanostructured and non-structured materials. It is conceivable that the introduction of the nanostructures often reduces the lifetime.

However, under concentration the situation is more favorable to the structured cells. While at one sun the advantage of the QWell cell for the conditions in Figure 4 is almost negligible, it may become about 3 percentage points (absolute), and even more for QWires, at 1000 suns. This advantage could be kept even for higher quality cells because the optimum efficiency of ideal cells at 1000 suns is obtained at a bandgap of around 1 eV (depending on the spectrum), below that of the GaAs.

However, if different quasi-Fermi levels can be maintained for band and confined electrons the efficiency for QDs can be much higher, exceeding the bulk cell in about 10 percentage points absolute. This good result requires the QD density to be much increased. With the present low concentration, the predictions of our model do not foresee any advantage. QD densities around $10^{17}\,\mathrm{cm}^{-3}$ seem feasible as discussed in Ref. 21. Also, the thickness of the QD layer could be increased. However, even with the present low density of QDs, better efficiency has already been recently achieved with a QD solar cell than with a similar one without QDs.[31] To interpret these results we have to assume a longer lifetime (which is thermodynamically possible) and a stronger light absorption. All this is possible and does not change the qualitative aspects discussed here.

ACKNOWLEDGMENTS

This work was supported by the European Commission through the FP7 project NG-CPV, the Spanish Science Ministry through the Project No. ENE2009-14481-C02-01 "Nanogeffes" and the Madrid Regional Government through S2009/ENE1477 "Numancia-2." We also thank Alexander Mellor for reviewing the manuscript.

[1]K. W. J. Barnham and G. Duggan, J. Appl. Phys. **67**, 3490 (1990).
[2]W. Guter, J. Schone, S. P. Philipps, M. Steiner *et al.*, Appl. Phys. Lett. **94**, 223504 (2009).
[3]R. R. King, A. Boca, W. Hong, X. Q. Liu *et al.*, paper presented at the 24th European Photovoltaic Solar Energy Conference and Exhibition, Hamburg, Germany, 21–25 September 2009.
[4]A. Luque, J. Appl. Phys. **110**, 031301 (2011).
[5]M. P. Lumb, M. Gonzalez, I. Vurgaftman *et al.*, Proc. SPIE **8256**, 82560S1–13 (2012).
[6]R. P. Raffaelle, S. Sinharoy, J. Andersen *et al.*, in *Proceedings of the 4th World Conference Photovoltaic Energy Conversion* (IEEE, NY, 2006), pp. 162–166.
[7]W. Shockley and H. J. Queisser, J. Appl. Phys. **32**(3), 510 (1961).
[8]G. L. Araújo and A. Martí, Sol. Energy Mater. Sol. Cells **33**, 213 (1994).
[9]A. Luque and A. Martí, Phys. Rev. Lett. **78**(26), 5014 (1997).
[10]A. Martí, L. Cuadra, and A. Luque, in *Proceedings of the 28th IEEE Photovoltaics Specialists Conference, Anchorage, USA, 15–22 September 2000* (IEEE, New York, 2000), p. 940.
[11]A. Luque, A. Martí, C. Stanley *et al.*, J. Appl. Phys. **96**(1), 903 (2004).
[12]S. M. Hubbard, C. D. Cress, C. G. Bailey *et al.*, Appl. Phys. Lett. **92**(12), 123512 (2008).
[13]V. Popescu, G. Bester, M. C. Hanna *et al.*, Phys. Rev. B **78**, 205321 (2008).
[14]R. Oshima, A. Takata, and Y. Okada, Appl. Phys. Lett. **93**(8), 083111 (2008).
[15]E. Antolín, A. Martí, P. G. Linares, I. Ramiro *et al.*, in *Proceedings of the 35th Photovoltaic Specialists Conference, Honolulu, USA, 20–25 June 2010* (IEEE, New York, 2010), p. 65.
[16]P. G. Linares, A. Martí, E. Antolín *et al.*, Solar Energy Materials and Solar Cells **98**, 240 (2012).
[17]A. Luque, A. Marti, and C. Stanley, Nature Photon. **6**, 146 (2012).
[18]A. M. Green, Prog. Photovoltaics **9**(2), 137 (2001).
[19]A. Luque, A. Martí, E. Antolín, P. G. Linares *et al.*, Sol. Energy Mater. Sol. Cells **95**, 2095 (2011).
[20]M. D. Ulrich, W. F. Seng, and P. A. Barnes, J. Comput. Electron. **1**, 431 (2002).
[21]A. Luque, A. Martí, E. Antolín, and P. G. Linares, Sol. Energy Mater. Sol. Cells **94**, 2032 (2010).
[22]A. Luque and A. Martí, IEEE Trans. Electron Devices **57**(6), 1201 (2010).
[23]A. Luque, P. G. Linares, E. Antolín, *et al.*, J. Appl. Phys. **111**, 044502 (2012).
[24]D. Zhou, G. Sharma, S. F. Thomassen, T. W. Reenaas, and B. O. Fimland, Appl. Phys. Lett. **96**, 061913 (2010).
[25]S. A. Blokhin, A. V. Sakharov, A. M. Nadtochy *et al.*, Semiconductors **43**, 514 (2009).
[26]C. G. Bailey, D. V. Forbes, R. P. Raffaelle, and S. M. Hubbard, Appl. Phys. Lett. **98**, 163105 (2011).
[27]S. M. Hubbard, C. G. Bailey, C. D. Cress *et al.*, in *Proceedings of the 33rd IEEE Photovoltaic Specialists Conference, San Diego, USA, 11–16 May 2008* (IEEE, New York, 2008), Vol. 1001.
[28]M. A. Green, K. Emery, Y. Hishikawa, W. Warta, and E. D. Dunlop, Prog. Photovoltaics **19**, 565 (2011).
[29]D. B. Bushnell, T. N. D. Tibbits, K. W. J. Barnham *et al.*, J. Appl. Phys. **97**, 124908 (2005).
[30]A. Luque, A. Martí, E. Antolín *et al.*, AIP Adv. **1**, 022125 (2011).
[31]C. G. Bailey, D. V. Forbes, S. J. Polly *et al.*, IEEE J. Photovoltaics **2**(3), 269 (2012).
[32]D. A. Clugston and P. A. Basore, in *Proceedings of the 26th IEEE Photovoltaic Specialists Conference, Anaheim, USA, 29 September–3 October 1997* (IEEE, New York, 1997), p. 207.
[33]A. G. Milnes, *Deep Impurities in Semiconductors* (John Wiley and Sons, NY, 1973).